ACS MEASUREMENT SCIENCE Au
AN OPEN ACCESS JOURNAL OF THE AMERICAN CHEMICAL SOCIETY

pubs.acs.org/measureau
Article

A Fast Immunosensor Based on Biohybrid Self-Assembled Nanostructures for the Detection of KYNA as a Cerebrospinal Fluid Biomarker for Alzheimer's Disease

A. Narváez,* J. Jiménez, M. Rodríguez-Núñez, M. Torre, E. Carro, M.-P. Marco, and E. Domínguez

Cite This: ACS Meas. Sci. Au 2025, 5, 242−249
Read Online

ABSTRACT: Although the role of kynurenic acid (KYNA) is not yet fully understood, recent research has implicated this tryptophan (Trp) metabolite as a significant biomarker in neurodegenerative diseases. In this study, we developed an immunosensor platform based on self-assembled polyelectrolyte multilayers (PEMs), employing an enzyme-labeled immunoreagent in a competitive displacement format that requires only a single wash step. This immunosensor enables the detection of KYNA and Trp with detection limits (LOD) of 9 pg/mL and 1.2 ng/mL, respectively. Results validated by traditional ELISA methods indicated elevated levels of KYNA and an increased KYNA/Trp ratio in the cerebrospinal fluid (CSF) of Alzheimer's patients compared to controls, consistent with previous findings. Additionally, this immunosensor platform can be readily adapted to detect other neuroactive Trp metabolites by substituting specific immunoreagents, supporting a flexible profile-based approach. This platform could serve as a rapid, cost-effective clinical tool for monitoring neurological and psychiatric disorders, potentially advancing therapeutic strategy development.

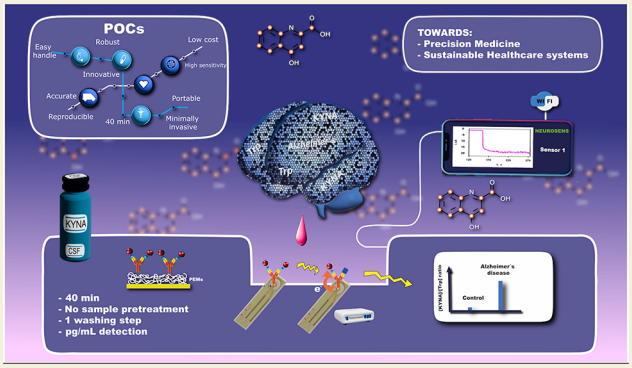

KEYWORDS: *KYNA, KYNA/Trp, electrochemical immunosensor, CSF, self-assembled polyelectrolyte multilayers*

Kynurenic acid (KYNA) has emerged as an important biomarker in cognitive impairment and dementia.[1,2] This bioactive compound is a product of tryptophan (Trp) metabolism via the kynurenine pathway (KP), which has a neuroprotective function under physiological conditions against other neurotoxic kynurenine metabolites synthesized during nicotinamide adenine dinucleotide (NAD^+) formation.

In pathological conditions including neurological and psychiatric disorders, there is an imbalance in the KP affecting the KYNA levels and elevating the production of neurotoxic metabolites such as 3-hydroxykynurenine (3-HK) and quinolinic acid (QUIN). The causes of this KP imbalance are still unclear. Some studies establish a link between Trp catabolism and the immune system in a bidirectional connection.[3] Kindler et al., have recently demonstrated the positive correlation between KP metabolites in the brain and plasma with an increase in inflammatory markers in schizophrenia disease.[4] An excess of KYN is produced in the periphery and converted into KYNA in the brain after crossing the blood-brain barrier (BBB) in the astroglia.[4] Additionally, inflammatory markers also stimulate the KP within macrophages, microglia, and dendritic cells to produce large quantities of QUIN, contributing to the neuroinflammatory environment.[1]

We recently demonstrated that both the concentration of KYNA and the KYNA/Trp ratio in cerebrospinal fluid (CSF) are elevated in patients with Alzheimer's disease (AD) compared to healthy subjects and other differentially diagnosed groups. This fact may indicate a compensatory mechanism in these AD patients based on its neuroprotective function, but also as an inflammatory response.[5] This work also showed how this AD-associated KYNA increase in CSF was not mirrored by an increase in the same inflammatory disease-specific blood ratio.[6−8]

The still incompletely understood role of KYNA as a biomarker would be better unraveled if a clinical tool was available for its direct and reliable detection in human fluids. This will greatly contribute to the understanding and monitoring of neurological and psychiatric disorders and, equally relevant, to the development of therapeutic strategies

Received: December 30, 2024
Revised: February 25, 2025
Accepted: February 25, 2025
Published: March 19, 2025

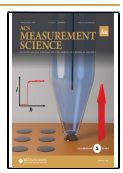

targeting KP to restore its imbalance. The KYNA analysis in biological matrices is usually performed by high-performance liquid chromatography (HPLC) coupled with electrochemical, fluorescent, or electrospray ionization detection.[9−11] Fluorescence detection has shown the highest sensitivity for KYNA in biological samples.[12]

On the other hand, immunological methods have been developed with the aim of being a routine analytical methodology. In this context, several enzyme-linked immunosorbent assay (ELISA) kits are commercially available for the detection of KYNA in serum, plasma, and other biological samples reaching detection limits in the ng/mL level. This is a relevant step toward simplification for clinical analysis, particularly regarding instrumentation. However, it remains tedious and expensive, involves critical washing steps, and requires specialized personnel and equipment.

Additional efforts toward low-cost and fast methods have resulted in miniaturized and automatized point-of-care (PoC) systems with different approaches developed for a multitude of analytes in biological samples.[13−16] In this line, the detection of KYNA has been approached with an electrochemical immunosensor based on two detection methods: chronoamperometry (CA) and impedance spectroscopy (EIS). The platform developed allows the detection of KYNA in an indirect format with limits of detection and quantitation in the pg/mL level, three orders of magnitude lower than the obtained with ELISA methodology. The performance of this platform was studied in spiked human serum samples, obtaining high sensitivity with an assay time of approximately 2 h.[17]

Finally, direct electrochemical detection on modified carbon paste electrodes has been demonstrated on doped blood samples but with detection limits above the target range.[18]

This study aims at a more efficient analytical platform in terms of protocols, skills, and instrumentation while preserving analytical properties. We disclose an analytical device for the electrochemical KYNA quantification as well as the KYNA/Trp ratio in biological samples in less than 40 min with no need for sample pretreatment. We claim that this is a significant step toward analytical simplification, enabling routine analysis of a relevant biomarker and showing a methodological pathway for additional biomolecules to be massively detected. This technology could be easily implemented for the delivery of PoC testing devices.

EXPERIMENTAL SECTION

Materials and Reagents

The sodium salt of 3-mercapto-1-propanesulfonic acid (MPS), poly(styrene sulfonic acid) (PSS) (MW 200, Fluka), kynurenic acid (KYNA), kynurenine (KYN) 5-hydroxy-L-tryptophan (5-HTP), L-tryptophan (Trp), quinolinic acid (QUIN), melatonin, serotonin (5-HT) and tryptamine, gold chloride tetrahydrate, IgG from rabbit serum, sodium citrate, Tween 20, and human Serum type AB were purchased from Sigma-Aldrich (Madrid, Spain). BST thick-film electrodes, BST-1212, (SPEAu) were provided by Bio Sensor Technologie GmbH (Berlin). Organic solvents (ethanol and acetonitrile), sodium hydroxide, polyethylene glycol, hydrogen peroxide (30%), and all buffer salts were obtained from Merck Millipore. The polyclonal antiserum anti-KYNA (As301), and the enzyme tracer (HRP-SIA-IHSH) were developed by the Nanobiotechnology for Diagnostics (Nb4D) group with the support of the Infraestructuras Cientifico-Tecnológicas Singulares (ICTS) "NANBIOSIS", more specifically by the Custom Antibody Service (CAbS, CIBER-BBN, IQAC−CSIC). Their preparation and characterization will be described elsewhere.[17] The tryptophan hydroxylase polyclonal antibody (ref PA5−19749) was purchased from Thermo Fisher Scientific, (Thermo Fisher Scientific, MA, USA) and the 5-hydroxy-L-tryptophan-HRP tracer was prepared according to the EZ-Link Plus activated Peroxidase protocol. IgG Antirabbit (R-3128) was purchased from Sigma-Aldrich (Madrid, Spain). The synthetic CSF was prepared by mixing 2.1 g NaCl, 0.07 g KCl, 0.08 g $CaCl_2$, 0.2 g glucose, 0.4 g $NaHCO_3$, and 2×10^{-3} g urea in a 250 mL Erlenmeyer flask (pH 7.4).[19,20] The gold nanoparticles were produced by the reduction under boiling conditions of a gold chloride tetrahydrate aqueous solution with sodium citrate, according to the previously reported procedures.[21]

The Osmium-based redox polymer Os(4,4′-dimethyl, 2,2′-bipyridine)2(l,10- phenanthroline, 5,6-dione) (Osphendione) mediator is synthesized according to procedures earlier published[22,23] and finally isolated as the PF6- salt form which was insoluble in aqueous solutions. It was ion-exchanged with an AG × 8 Cl^- form (BIORAD) ion-exchange resin to yield the water-soluble form of the positively charged redox polymer used in electrochemical experiments.

Apparatus

The electrochemical measurements were performed in a conventional three-electrode cell using a computer-controlled ECO Chemie Autolab PSTAT 10 potentiostat. Potentials were measured against a potassium-saturated silver: silver chloride electrode (Ag/AgCl, KCl_{sat}) and a coiled Pt wire served as the counter electrode.

Scanning Electron Microscopy (SEM) was performed using a DSM950 Zeiss (Karl Zeiss, Oberkochen, Germany) with dried samples either coated with gold via evaporation or sputtered. Finally, the average particle size of gold nanoparticles was determined by Dynamic Light Scattering using a Microtac UPA 150 (Leeds and Northrup, Ireland).

Immunosensor Platform

The immunosensor was constructed according to the previously described work.[24] Briefly, the SPEAu (geometric area ca. 1.0 ± 0.2 mm^2) were electrochemically cleaned by repetitive cyclic voltammogram from −0.05 to 1.2 V at 150 mV s^{-1} in a solution of 4×10^{-2} mM H_2SO_4 until a characteristic clean gold cyclovoltammogram was obtained (approx. 100 cycles).

In the first step, the electrodes were modified with 2.5 nM gold colloids, a solution of particles with a monodisperse size distribution of 18.1 ± 0.9 nm in diameter (n = 100), as measured by particle analyzer and SEM images (Supporting Information: Figure S1A,B). Afterward, a first negatively charged monolayer (Au@AuNP/MPS) was obtained after the electrode incubation in MPS, 0.2 mg/mL dissolved in a 50% ethanolic solution, at room temperature for 12 h. Then, the supramolecular architecture was built up by sequential deposition of layers of a positively charged redox polymer (RP, 2 h from a 1 mg/mL aqueous solution) intercalated with a negatively charged polyelectrolyte (PSS, 15 min with a 50 mg/L aqueous solution), in a final configuration Au@AuNP/MPS/RP/PSS/RP. After the self-assembly of each layer, the electrodes were rinsed with Milli-Q water. Then, the appropriate antibody was deposited by its incubation in 0.05 M carbonate buffer pH 8.9 for 20 min. After rinsing with Milli-Q water, the corresponding enzyme tracer was immobilized by affinity reaction (30 min at 25 °C without stirring, dissolved in 0.1 M phosphate buffer pH 7.0). Finally, these modified gold electrodes were stored overnight at 4 °C. Prior to the electrochemical measurements, the electrodes were rinsed with Tween 20, 0.05% v/v to reduce nonspecific response.

Electrochemical Measurements

The immunosensor was designed to operate by displacement in a competitive format and a single washing step with a final configuration: Au@AuNP/MPS/RP/PSS/RP/Ab/Ag-HRP*. The presence of the analyte (incubation for 30 min) displaces the HRP labeled tracer decreasing the immunosensor response proportionally to the analyte concentration. A scheme of the displacement assay is shown in Figure 1.

https://doi.org/10.1021/acsmeasuresciau.4c00102
ACS Meas. Sci. Au 2025, 5, 242−249

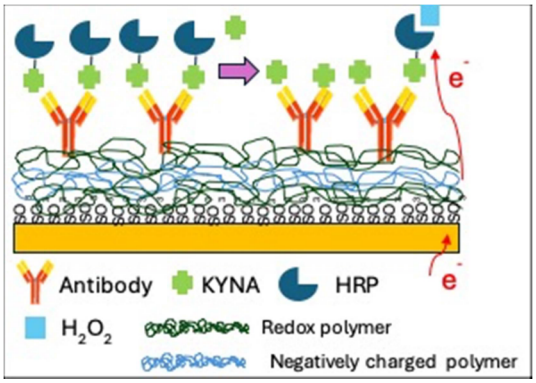

Figure 1. Schematic representation of the electrochemical immunosensor configuration for the detection of KYNA based on self-assembled polyelectrolyte multilayers.

The electrochemical response was evaluated by amperometry at a constant potential (50 mV versus Ag/AgCl, KCl_{sat}), stirred in 0.1 M phosphate buffer solution pH 7.0, and after the addition of H_2O_2 solution. The final substrate concentration was 250 μM.

RESULTS AND DISCUSSION

The core idea was to develop a PoC device based on biohybrid supramolecular nanostructures for the electrochemical detection of KYNA in CSF.

Characterization of the Immunosensor Platform

The initial nanoparticle layer, Au@AuNP, was constructed to increase the electroactive area of the gold paste; after deposition of the gold nanoparticles, the electroactive area of the sensors was increased by a factor of 1.5 (n = 86), as evidenced by the increase in the area of the gold oxide reduction peak (from $6.4 \pm 1.5 \times 10^{-10}$ to $9.5 \pm 1.1 \times 10^{-10}$ C/cm^2). After drying the electrode, the surface was subsequently functionalized with biohybrid growth layers as described in the experimental section.

Subsequently, a monolayer of MPS was deposited to create a negatively charged surface that would allow the deposition of a positively charged redox polymer. This redox architecture (Au@AuNP/MPS/RP) exhibits a cyclovoltamperogram characteristic of this class of osmium-based polymers with a surface coverage of $5.5 \pm 0.3 \times 10^{-10}$ mol/cm^2 calculated by integrating the anodic peak of the cyclovoltamperograms performed at 50 mV s^{-1}. A second layer of RP was deposited through an intermediate layer of PSS, (Au@AuNP/MPS/RP/PSS/RP) allowing us to increase the redox coverage layer by a factor of 2.6 and up to $10 \pm 1 \times 10^{-10}$ mol/cm^2 while maintaining the conditions of electrochemical reversibility (Supporting Information Figure S2). Finally, the deposition of the antibody and HRP tracer was carried out as described in the experimental section (Au@AuNP/MPS/RP/Ab/Ag-HRP*).

The deposition of the different layers described above was followed by the SEM technique, which allowed us to observe the morphological surface changes associated with the deposition of the layers. Figure 2 shows the SEM images for the platform Au@AuNP/MPS/RP/Ab/Ag-HRP*, (A) shows a typical clean electrode surface followed by (B) the deposition of the Au-colloids and (C) a self-assembled nondensely packed monolayer of MPS that covers the entire gold surface as described elsewhere.[25]

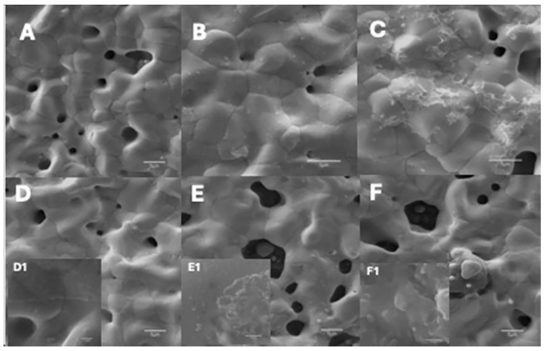

Figure 2. SEM images of the Immunosensor platform: (A) SPEAu naked (B) gold colloids deposited on SPEAu (Au@AuNP) (C) MPS layer (Au@AuNP/MPS), (D) redox polymer layer and inner imagen (D1) the edge where the polymer layer ends, (Au@AuNP/MPS/RP), (E and E1) the Ab layer (Au@AuNP/MPS/RP/Ab) and finally (F and F1) the HRP-tracer layer (Au@AuNP/MPS/RP/Ab/Ag-HRP*).

The deposition of a positively charged redox polymer results in a homogeneous surface (D) while the ulterior deposition of the antibody (a globular molecule) and the HRP tracer increased the rugosity and heterogeneity, as can be seen in the insets of Figure 2E,F. These changes in the morphology are similar to those found when a polymer and a globular protein are sequentially and successfully immobilized onto an electrode surface.[26]

The configuration of this platform is based on a competitive displacement assay, where the balance between the dissociation and affinity kinetics of the immunocomplexes, as well as the loading of the immobilized immunoreagent, become determinants for the sensitivity, linear range, and selectivity of the platform.[27] Therefore, the loading of the two immunoreagents was studied. It was considered that pursuing the highest electrochemical communication of the HRP tracer with the electrode surface was the best indicator for the optimization of the analytical response, considering the inherent insulator properties of the antibody layer. Consequently, the electrochemical response efficiency was optimized by analyzing the percentage of HRP tracer electrochemically communicated with the electrode within this architecture through the redox polymer, by adding catechol as a soluble mediator after the H_2O_2 response. The signal increase upon the addition of the soluble mediator would represent a poorly communicated HRP tracer and thus, the ratio between the initial response to H_2O_2 and the obtained after the addition of catechol would be an indicator of the efficient redox communication.[28] As can be seen in Figure S3, a combination of 1 pg/mL for the antibody concentration and 4 ng/mL of HRP tracer showed the most efficient communication. According to our results, this relationship between the antibody (protein-insulator) and the tracer could be extrapolated to any pair of immunoreagents to be used in the future for any immunosensor developed with this displacement configuration as long as they exhibit appropriate relative affinities for the displacement assay.

Blank electrodes (immobilizing a similar antibody at the same concentration but specific to dexamethasone) were used to assess the nonspecific response of the electrodes. The response obtained was in the same range as that previously obtained for the highest KYNA concentrations (33% of total response), with all tracers displaced. In this sense, the addition of BSA to reduce the nonspecific adsorption by blocking the

https://doi.org/10.1021/acsmeasuresciau.4c00102
ACS Meas. Sci. Au 2025, 5, 242−249

uncovered electrode surface resulted in a decrease in the nonspecific response but also a decrease in the maximum signal, as expected after deposition of an insulator protein blocking electron transfer between redox polymer and HRP tracer. Nevertheless, this effect is minimized through the normalization of the values, which helps to mitigate its impact on the loss of sensitivity.

Operational Characterization

Once the Au@AuNP/MPS/RP/Ab/Ag-HRP* configuration had been characterized, the immunosensor was incubated with the standards, as shown in the calibration curve in Figure 3.

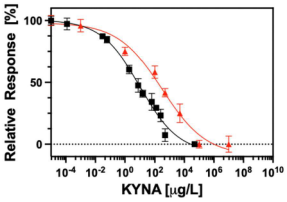

Figure 3. Representative calibration curve of KYNA redox-immunosensor by a displacement competitive assay (red) and the traditional ELISA format by a competitive (two steps) format in black. 250 μM H_2O_2, 0.1 M phosphate buffer, pH 7.0, 27 °C. E_{appl}: 50 mV vs Ag/AgCl, KCl_{sat}. Each calibration point was measured in duplicates. The ELISA calibration curve was measured at 650 nm after the addition of the appropriate substrate.

Compared with the traditional ELISA technique, we can observe that the simplification of the assay format is concomitant with a significant increase in the IC_{50}, although the platform maintains analytical performance with a LOD of 0.06 ± 0.02 μg/L, calculated as 90% of the response, and a linear range (LR) from 1.4 to 1.1 × 10^4 μg/L.

The cross-reactivity (CR) of different molecules derived from the Trp pathway was determined (CR: calculated according to the equation CR (%) = IC50(analyte)/IC50-(cross-reactant) × 100). The results demonstrated that the immunosensor exhibits the same specificity profile as the ELISA technique, maintaining a cross-reactivity (CR) below 0.01% for the analogous components (Trp, L-kynurenine, 5-THP, 5-HT, and melatonin).

Determination of KYNA in Complex Matrices

In order to assess the matrix effect, we approached the study of the immunosensor in complex biological matrices by constructing calibration curves in undiluted matrices. The same range of KYNA concentrations was used for all of the matrices. As can be seen in Figure 4 and Table 1, all assays showed similar analytical features, although there is a clear decrease in the maximum signal when human serum is used as a matrix, probably due to the "endogenous" KYNA content and the passivation of the electrode surface.

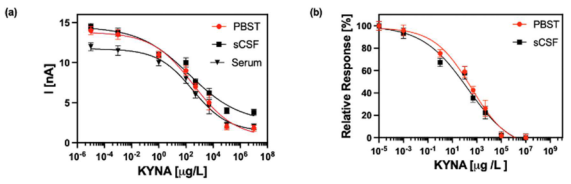

Figure 4. Calibration curves of the immunosensor for the detection of KYNA (a) in buffer (PBST- pH: 6.5, red color), undiluted sCSF (black color), and undiluted human serum (black triangle) in optimal conditions (b) same calibration curves but without serum. Each calibration point was measured in triplicates.

The developed immunoplatform enables the detection of KYNA in complex matrices with a LOD of 9 pg/mL in synthetic CSF (sCSF), significantly lower than the optimal cutoff reported in the literature for KYNA metabolites in sCSF, which was established at 7.5 ng/mL by immunoassay[9] or those described by HPLC with spectrophotometric, fluorimetric or MS detection, ranging from 189 to 946 pg/mL[29−32] The detected value in sCSF of 9 pg/mL is well below those described as normal levels in CSF, (0.19−3 ng/mL), with this physiological value greatly depending on the various regulated events involved in KYNA metabolism and also according to the technique used in the quantification.[5,33,34]

It is worth mentioning that when the sCSF matrix is used, there are no significant differences compared to the buffer, although a slight decrease in IC_{50} can be observed (IC_{50} 179 μg/L). This decrease is not noticeable in the case of serum (359 μg/L in buffer vs 321 μg/L in serum). When serum was used as a matrix, the LOD obtained was similar to that of the unique electrochemical immunosensor described in the literature for KYNA detection, which was 62 ng/L in comparison with the 100 ng/L in undiluted serum reported here and with the added advantage of reducing the time of the assay up to 95 min and the number of steps.[17]

All assayed matrices showed an increase in the nonspecific response, with this effect being more noticeable for sCSF. However, the nonspecific adsorption due to this matrix was negligible in the ELISA configuration, presuming that the ionic nature of the matrix can affect the analytical properties of the developed immunosensor (LOD and linear range, see Supporting Information Figure S4). However, the sensor retains sufficient integrity and analytical properties to be used for the detection of analytes in complex matrices.

Replicability and Reproducibility of the Immunosensor Platform

The robustness of the developed concept was evaluated through its replicability and reproducibility using three different levels of KYNA concentration, low (IC_{80}), medium (IC_{50}), and high (IC_{20}) in sCSF. In all cases, the platform was prepared manually as described in the Experimental section meaning that no single deposition step was automatically performed. The replicability is expressed as the percentage of the coefficient of variation (CV) for a set of three electrodes prepared by one person on a given day, while reproducibility includes the preparation by a second researcher not well acquainted with the preparation and use of the electrodes.

The replicability of the immunosensors remained acceptable with CV values of 3.6, 6.0, and 10% for the IC_{80}, IC_{50}, and IC_{20}, respectively, obtaining values similar to those reported in the literature for immunoassays.[35,36] However, this was highly dependent on the expertise achieved in the electrode preparation because the CV obtained when the electrodes were prepared by a different researcher was above 80% for low (IC_{80}) and high concentrations (IC_{20}), while the CV at the IC_{50} level was 22%. The manufacturing of these electrodes is expected to be automatic by successive layer deposition as no need for any chemistry and thus, no significant variations are expected in their preparation.

https://doi.org/10.1021/acsmeasuresciau.4c00102
ACS Meas. Sci. Au 2025, 5, 242−249

Table 1. Analytical Features of the Immunosensor for the Detection of KYNA in Different Undiluted Synthetic Matrices

metric	PBST[a]	sCFS	serum
I_{min} (nA)	0.6 ± 1.1	2.5 ± 1.6	1.4 ± 0.6
I_{max} (nA)	13.8 ± 0.6	14.5 ± 0.9	11.7 ± 0.4
slope	−0.3.5 ± 0.07	−0.23 ± 0.08	−0.34 ± 0.06
IC_{50} μg/L	359 ± 2	179 ± 4	321 ± 2
linearrange μg/L	1.4 to 1.1 × 10^4	0.27 to 8.8 × 10^3	0.27 to 8.1 × 10^3
LOD μg/L	0.07 ± 0.02	0.009 ± 3 × 10^{-3}	0.1 ± 0.1
R^2	0.98	0.97	0.99

Assessment of the Immuno-Platform with Clinical Samples

To further evaluate the accuracy of the developed immunosensor, and considering the absence of interference when using CSF as the matrix, six CSF samples from diagnosed Alzheimer's disease patients and healthy subjects were simultaneously tested using the developed immunosensor and the traditional ELISA technique, as described in our previous work.[5]

The CSF samples provided by Prof. Carro of the Neurodegenerative Diseases Group, Hospital 12 de Octubre Research Institute (*i* mas12) were analyzed as a proof of concept (Table 2).

Table 2. Clinical Parameters of the Selected Samples

ID	sex	age	onset (months)	MMSE[a]
AD212	M	74	36	20
AD214	F	73	24	23
AD215	F	69	24	22
C145	F	71		
C154	F	66		
C156	M	58		

[a]MMSE, mini-mental state examination.

As can be seen in Figure 5, there is a good correlation between the results obtained by the platform and the ELISA assay.

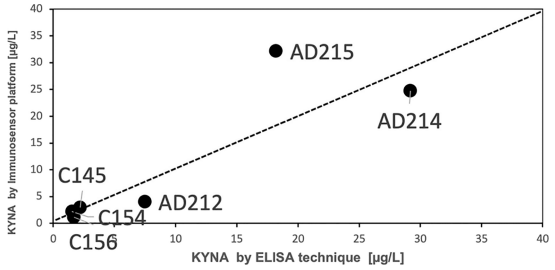

Figure 5. Graph showing the correlation among the ELISA format and the developed immunosensor platform for KYNA detection in CSF samples.

The slope of 1.08 is very close to 1.0, and the regression coefficient was 0.87. The differences can be attributed to the different format of the assay and its reflection in the CR.

Additionally, since KYNA is a product of Trp metabolism via KP, a major motivation for the measurement of Trp here is to adopt a representation based on the KYNA/Trp ratio that is an indicator of the activity of kynurenine aminotransferases (KATs) in its degradation pathway. So, taking advantage of the versatility of this configuration, we proceeded to construct an electrochemical immunosensor to detect Trp, maintaining the immobilization conditions with the appropriate immunoreagents in the same conditions. The corresponding calibration curve is shown in Figure 6.

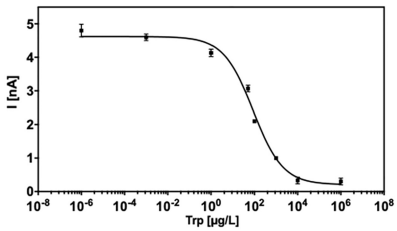

Figure 6. Representative calibration curve of electrochemical Trp immunosensor by a displacement competitive assay; 250 μM H_2O_2 phosphate buffer 0.1 M, pH 7.0, 27 °C. E_{appl}: 50 mV vs Ag/AgCl, KClsat. Each calibration point was measured in triplicates.

As can be seen, the immunosensor presents the following analytical features: an IC_{50} of 86 ± 1.5 μg/L, a dynamic range of 6−117 μg/L and a LOD of 1.1 ± 0.5 μg/L. The CR studies showed a high recognition for Trp and interference of melatonin of 6%, and less interference <0.01% for the rest of analogue analytes as, 5-HT, and KYNA.

The results obtained with the new immunosensor indicated no significant differences between patients diagnosed with Alzheimer's disease and healthy subjects ($t(5\%) = 2.8$, $p = 0.8$). These findings are consistent with previous studies, which also found no differences in CSF Trp levels between AD patients and controls based on ELISA measurements.[5]

For the KYNA/TRP ratio, the results showed a strong correlation with a slope of 1.1 and a correlation coefficient of 0.79.

However, the correlation was weaker in samples from Alzheimer's disease patients. Nevertheless, an increase in the KYNA/Trp ratio in the CSF of Alzheimer's disease patients compared to controls was observed, consistent with previous findings (Figure 7).

The observed deviations from a value of 1 in the slope, when comparing the two detection methods, can be attributed to the change in the immunoassay format. While this change does not alter the CR profiles, it may influence measurements in Alzheimer's patients, where the differential expression of Trp metabolites is more pronounced.

Finally, to assess the storage stability of the electrodes, the maximum amperometric response was measured in a series of immunosensors stored in dry conditions and at 4 °C for 5 months. As can be seen in Figure 8, the initial maximum response remains stable for up to 8 weeks, when stability begins to vary between batches, although the response remains above 90%. However, this storage stability is much higher than that reported in the literature for multilayers, where the

https://doi.org/10.1021/acsmeasuresciau.4c00102
ACS Meas. Sci. Au 2025, 5, 242−249

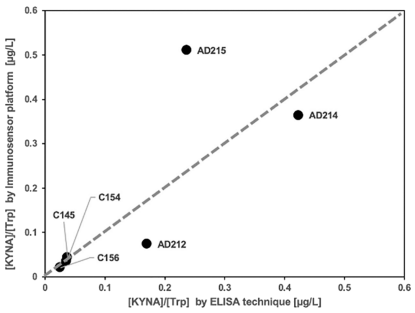

Figure 7. Graph showing the correlation among the ELISA format and the developed immunosensor platform for the KYNA/Trp ratio in CSF samples.

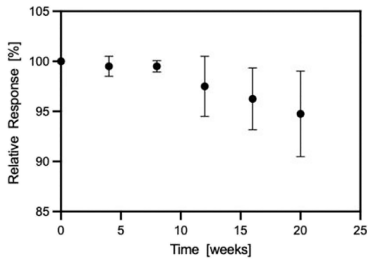

Figure 8. Evaluation of long-term storage of the developed immunosensors based on PEMs.

response decreases by approximately 20% from 4 to 7 weeks.[37−39]

With this work, we have demonstrated, as a proof of concept, the possibility of using PoC systems for the detection of KP metabolites in human CSF without sample pretreatment. However, further studies with a high number of samples should be carried out, as well as better optimization in order to improve the repeatability at high concentrations, which can affect the accuracy of the developed immunosensors.

CONCLUSIONS

We have developed a universal immunosensor platform for the electrochemical quantification of KYNA as well as the KYNA/Trp ratio in biological fluids such as CSF in less than 40 min and without having to pretreat the samples. The portable system shows an LOD for KYNA of 9.0 ng/L in CSF with the appropriate analytical characteristics.

Sequential construction of this supramolecular architecture based on self-assembled multilayers, Au@AuNP/MPS/RP/PSS/RP/Ab/Ag-HRP*, was followed by the corresponding morphological changes by SEM and electrochemical techniques. The results showed an ordered multilayer architecture that optimizes the deposition of biomolecules as antibodies and enzyme tracers. This allows an immunosensor based on a displacement format assay.

This format simplifies the procedures of the PoC developed with fewer washing steps, which results in reducing the time analysis as compared with other immunosensors in the literature. The resulting configuration was validated by the traditional ELISA assay showing good correlations as KYNA concentration and as KYNA/Trp ratio with slopes and correlation coefficients close to 1.0 (1.1 for KYNA/Trp ratio) and 0.9 (0.8 for KYNA/Trp ratio), respectively. The results obtained showed, in agreement with our previous results, an increase of KYNA and KYNA/Trp ratio in the CSF of Alzheimer's disease patients compared to controls. To the best of our knowledge, this is the first immunosensor or sensor capable of directly quantifying KYNA in real samples, specifically in cerebrospinal fluid (CSF), without requiring any prior sample treatment. Unlike other methods that require extensive sample dilution—often leading to significant analyte loss—our approach eliminates the need for any sample treatment, allowing for the detection and accurate quantification of the low concentrations of KYNA naturally present in CSF. This system represents a significant advancement in the field, offering a more practical and efficient solution for clinical and analytical applications.

In this sense, the ability to detect KYNA levels in CSF in 40 min at low cost opens up new opportunities to understand the role of these KP metabolites in neurological and psychiatric disorders and develop therapeutic strategies based on specific biomarkers associated with these diseases. In addition, this immunosensor platform can be easily implemented and extended to other neuroactive Trp metabolites by changing only the immunoreagents presented in a profile immunosensor platform.

ASSOCIATED CONTENT

Supporting Information

The Supporting Information is available free of charge at https://pubs.acs.org/doi/10.1021/acsmeasuresciau.4c00102.

Figure S1A: Histogram of the size distribution of the synthesized gold nanoparticles determined using a Microtac UPA 150 ultrafine particle analyzer; Figure S1B: (B) SEM image of a gold colloid isolated on the surface of the electrode; Figure S2: Voltammetric response of one layer (a) and two layers (b) of Osmium-redox polymer (RP) self-assembled; measurements were obtained at a scan rate of 50 mV s^{-1} in 0.1 M phosphate buffer pH 7.0 vs Ag/AgCl, KClsat; Figure S3: Efficiency of the electrochemical response as a function of the concentration of the antibody (A) and the HRP tracer (B); Figure S4: ELISA format calibration curves for detecting KYNA in buffer (PBST- pH:6.5 red color) and undiluted sCSF (black color) under optimal conditions; and each calibration point was measured in triplicate (PDF)

AUTHOR INFORMATION

Corresponding Author

A. Narváez − *Bioanalysis and Biosensor group, University of Alcalá, 28805 Alcalá de Henares, Spain;* orcid.org/0000-0001-8141-558X; Email: arantzazu.narvaez@uah.es

Authors

J. Jiménez − *Bioanalysis and Biosensor group, University of Alcalá, 28805 Alcalá de Henares, Spain*

M. Rodríguez-Núñez − *Surfactants and Nanobiotechnology Department, Nanobiotechnology for Diagnostics (Nb4D) Group, Institute for Advanced Chemistry of Catalonia (IQAC) of the Spanish National Research Council (CSIC), 08034 Barcelona, Spain; CIBER de Bioingeniería, Biomateriales y Nanomedicina (CIBER-BBN), Instituto de Salud Carlos III (ISCIII), 28029 Madrid, Spain*

M. Torre − *Bioanalysis and Biosensor group, University of Alcalá, 28805 Alcalá de Henares, Spain*

https://doi.org/10.1021/acsmeasuresciau.4c00102
ACS Meas. Sci. Au 2025, 5, 242−249

E. Carro − *Group of Neurodegenerative Diseases, Hospital 12 de Octubre Research Institute (imas12), 28041 Madrid, Spain; CIBER de Enfermedades Neurodegenerativas (CIBERNED)s, Instituto de Salud Carlos III (ISCIII), 28029 Madrid, Spain;* Present Address: Neurobiology of Alzheimer's disease Unit, Functional Unit for Research into Chronic Diseases, Instituto de Salud Carlos III, 28029 Madrid, Spain

M.-P. Marco − *Surfactants and Nanobiotechnology Department, Nanobiotechnology for Diagnostics (Nb4D) Group, Institute for Advanced Chemistry of Catalonia (IQAC) of the Spanish National Research Council (CSIC), 08034 Barcelona, Spain; CIBER de Bioingeniería, Biomateriales y Nanomedicina (CIBER-BBN), Instituto de Salud Carlos III (ISCIII), 28029 Madrid, Spain;* orcid.org/0000-0002-4064-1668

E. Domínguez − *Bioanalysis and Biosensor group, University of Alcalá, 28805 Alcalá de Henares, Spain;* Present Address: Spanish National Research Council, (CSIC), 28006 Madrid, Spain.

Complete contact information is available at: https://pubs.acs.org/10.1021/acsmeasuresciau.4c00102

Author Contributions

A.N.: Writing−original draft, Data curation, Conceptualization, Review & editing. Funding acquisition. J.J.: Investigation, Data curation. M.R.-N.: Investigation, Data curation. Review & editing. M.T.: Review & editing. Supervision, Project administration. E.C.: Provision of the clinical CSF samples used. Conceptualization, Supervision. M.-P.M.: Conceptualization, Supervision, Resources, Project administration, Funding acquisition. E.D.: Data curation. review and editing, Supervision, Methodology. Funding acquisition

Funding

This work is supported by the Spanish Ministry for Science, Innovation and Universities through PID2021−126257OB-C22 project.

Notes

The authors declare no competing financial interest.

■ ACKNOWLEDGMENTS

This work is supported by the Spanish Ministry for Science, Innovation and Universities through PID2021-126257OB-C22 project.

■ ABBREVIATIONS

3-HK, 3-hydroxykynurenine; 5-HT, serotonin; 5-HTP, 5-hydroxy-L-tryptophan; AD, Alzheimer's disease; AuNP, gold colloids; CA, chronoamperometry; CR, cross-reactivity; CSF, cerebrospinal fluid; CV, coefficient of variation; CV, cyclovoltammetry; EIS, impedance spectroscopy; ELISA, enzyme-linked immunosorbent assay; HPLC, high-performance liquid chromatography; HRP, horse radish peroxidase; KATs, kynurenine aminotransferases; KP, kynurenine pathway; KYN, kynurenine; KYNA, kynurenic acid; LOD, detection limit; LR, linear range; MMSE, mini-mental state examination; MPS, 3-mercapto-1-propanesulfonic acid; NAD^+, nicotinamide adenine dinucleotide; PEMs, self-assembled polyelectrolyte multilayers; PoC, point-of-care testing; PSS, poly(styrene sulfonic acid; QUIN, quinolinic acid; RP, osmium based redox polymer; SAMs, self-assembled polyelectrolyte Monolayers; sCFS, synthetic cerebrospinal fluid; SEM, scanning electron microscopy; SPE-Au, BST thick-film electrodes, BST-1212; Trp, L-tryptophan

■ REFERENCES

(1) Ostapiuk, A.; Urbanska, E. M. Kynurenic acid in neurodegenerative disorders-unique neuroprotection or double-edged sword? *Cns Neuroscience & Therapeutics* **2022**, *28* (1), 19−35.
(2) Hestad, K.; Alexander, J.; Rootwelt, H.; Aaseth, J. O. The Role of Tryptophan Dysmetabolism and Quinolinic Acid in Depressive and Neurodegenerative Diseases. *Biomolecules* **2022**, *12* (7), 998.
(3) Davidson, M.; Rashidi, N.; Nurgali, K.; Apostolopoulos, V. The Role of Tryptophan Metabolites in Neuropsychiatric Disorders. *Int. J. Mol. Sci.* **2022**, *23* (17), 9968.
(4) Kindler, J.; Lim, C. K.; Weickert, C. S.; Boerrigter, D.; Galletly, C.; Liu, D.; Jacobs, K. R.; Balzan, R.; Bruggemann, J.; O'Donnell, M.; et al. Dysregulation of kynurenine metabolism is related to proinflammatory cytokines, attention, and prefrontal cortex volume in schizophrenia. *Molecular Psychiatry* **2020**, *25* (11), 2860−2872.
(5) Gonzalez-Sanchez, M.; Jimenez, J.; Narvaez, A.; Antequera, D.; Llamas-Velasco, S.; Herrero-San Martin, A.; Arjona, J. A. M.; de Munain, A. L.; Bisa, A. L.; Marco, M. P.; et al. Kynurenic Acid Levels are Increased in the CSF of Alzheimer's Disease Patients. *Biomolecules* **2020**, *10* (4), 571.
(6) Moulin, D.; Millard, M.; Taïeb, M.; Michaudel, C.; Aucouturier, A.; Lefèvre, A.; Bermúdez-Humarán, L. G.; Langella, P.; Sereme, Y.; Wanherdrick, K.; et al. Counteracting tryptophan metabolism alterations as a new therapeutic strategy for rheumatoid arthritis. *Annals of the Rheumatic Diseases* **2024**, *83* (3), 312.
(7) Roberts, I.; Wright Muelas, M.; Taylor, J. M.; Davison, A. S.; Winder, C. L.; Goodacre, R.; Kell, D. B. Quantitative LC−MS study of compounds found predictive of COVID-19 severity and outcome. *Metabolomics* **2023**, *19* (11), 87.
(8) Zhen, D. L.; Liu, J. J.; Zhang, X. D.; Song, Z. H. Kynurenic Acid Acts as a Signaling Molecule Regulating Energy Expenditure and Is Closely Associated With Metabolic Diseases. *Frontiers in Endocrinology* **2022**, *13*, 10.
(9) Zhao, J. X.; Chen, H.; Ni, P. H.; Xu, B. X.; Luo, X. M.; Zhan, Y. M.; Gao, P. J.; Zhu, D. L. Simultaneous determination of urinary tryptophan, tryptophan-related metabolites and creatinine by high performance liquid chromatography with ultraviolet and fluorimetric detection. *Journal of Chromatography B-Analytical Technologies in the Biomedical and Life Sciences* **2011**, *879* (26), 2720−2725.
(10) Bao, Y.; Luchetti, D.; Schaeffer, E.; Cutrone, J. Determination of kynurenic acid in rat cerebrospinal fluid by HPLC with fluorescence detection. *Biomedical Chromatography* **2016**, *30* (1), 62−67.
(11) Liu, R.; Zhao, X.; Geng, G.; Lai, Y. Development and validation of an LC-MS/MS method to quantify kynurenic acid in human plasma. *Bioanalysis* **2022**, *14* (20), 1327−1336.
(12) Wennstrom, M.; Nielsen, H. M.; Orhan, F.; Londos, E.; Minthon, L.; Erhardt, S. Kynurenic Acid Levels in Cerebrospinal Fluid from Patients with Alzheimer's Disease or Dementia with Lewy Bodies. *Int. J. Tryptophan Res.* **2014**, *7*, 1−7.
(13) Rosa, B. G.; Akingbade, O. E.; Guo, X. T.; Gonzalez-Macia, L.; Crone, M. A.; Cameron, L. P.; Freemont, P.; Choy, K. L.; Guder, F.; Yeatman, E.; et al. Multiplexed immunosensors for point-of-care diagnostic applications. *Biosens. Bioelectron.* **2022**, *203*, No. 114050.
(14) Piorino, F.; Patterson, A. T.; Styczynski, M. P. Low-cost, point-of-care biomarker quantification. *Curr. Opin. Biotechnol.* **2022**, *76*, No. 102738.
(15) Wang, H.; Tang, J.; Wan, X.; Wang, X.; Zeng, Y.; Liu, X.; Tang, D. Mechanism Exploration of the Photoelectrochemical Immunoassay for the Integration of Radical Generation with Self-Quenching. *Anal. Chem.* **2024**, *96* (38), 15503−15510.
(16) Wang, Y.; Zeng, R.; Tian, S.; Chen, S.; Bi, Z.; Tang, D.; Knopp, D. Bimetallic Single-Atom Nanozyme-Based Electrochemical-Photo-

thermal Dual-Function Portable Immunoassay with Smartphone Imaging. *Anal. Chem.* **2024**, *96* (33), 13663−13671.
(17) Marrugo-Ramirez, J.; Rodriguez-Nunez, M.; Marco, M. P.; Mir, M.; Samitier, J. Kynurenic Acid Electrochemical Immunosensor: Blood-Based Diagnosis of Alzheimer's Disease. *Biosensors-Basel* **2021**, *11* (1), 20.
(18) Bornaei, M.; Khajehsharifi, H.; Shahrokhian, S.; Sheydaei, O.; Zarnegarian, A. Differential pulse voltammetric quantitation of kynurenic acid in human plasma using carbon-paste electrode modified with metal-organic frameworks. *Mater. Chem. Phys.* **2023**, *295*, No. 127016.
(19) Hawk, P. B.; Oser, B. L. *Hawk's physiological chemistry*; Blakiston Division; McGraw-Hill, 1965.
(20) Zhang, F.; Yang, L.; Bi, S.; Liu, J.; Liu, F.; Wang, X.; Yang, X.; Gan, N.; Yu, T.; Hu, J. Neurotransmitter dopamine applied in electrochemical determination of aluminum in drinking waters and biological samples. *J. Inorg. Biochem.* **2001**, *87* (1−2), 105−113.
(21) Frens, G. Controlled Nucleation for the Regulation of the Particle Size in Monodisperse Gold Suspensions. *Nature Physical Science* **1973**, *241* (105), 20−22.
(22) Katakis, I.; Ye, L.; Heller, A. Electrostatic Control of the Electron-Transfer Enabling Binding of Recombinant Glucose Oxidase and Redox Polyelectrolytes. *J. Am. Chem. Soc.* **1994**, *116* (8), 3617−3618.
(23) Amouyal, E.; Homsi, A.; Chambron, J.-C.; Sauvage, J.-P. Synthesis and study of a mixed-ligand ruthenium(II) complex in its ground and excited states: bis(2,2′-bipyridine)(dipyrido[3,2-a: 2′,3′-c]phenazine-N4N5)ruthenium(II). *J. Chem. Soc., Dalton Trans.* **1990**, *6*, 1841−1845.
(24) Dominguez, E.; Suarez, G.; Narvaez, A. Electrostatic assemblies for bioelectrocatalytic and bioelectronic applications. *Electroanalysis* **2006**, *18* (19−20), 1871−1878.
(25) Mokrani, C.; Fatisson, J.; Guérente, L.; Labbé, P. Structural Characterization of (3-Mercaptopropyl) sulfonate Monolayer on Gold Surfaces. *Langmuir* **2005**, *21* (10), 4400−4409.
(26) Derkus, B.; Cebesoy Emregul, K.; Mazi, H.; Emregul, E.; Yumak, T.; Sinag, A. Protein A immunosensor for the detection of immunoglobulin G by impedance spectroscopy. *Bioprocess Biosyst. Eng.* **2014**, *37* (5), 965−976.
(27) Khor, S. M.; Thordarson P, Fau; Gooding, J. J.; Gooding, J. J. The impact of antibody/epitope affinity strength on the sensitivity of electrochemical immunosensors for detecting small molecules. *Anal. Bioanal. Chem.* **2013**, *405*, 3889−3998.
(28) Tang, D.; Yuan, R.; Chai, Y. Electron-Transfer Mediator Microbiosensor Fabrication Based on Immobilizing HRP-Labeled Au Colloids on Gold Electrode Surface by 11-Mercaptoundecanoic Acid Monolayer. *Electroanalysis* **2006**, *18* (3), 259−266.
(29) Flieger, J.; Swiech-Zubilewicz, A.; Sniegocki, T.; Dolar-Szczasny, J.; Pizon, M. Determination of Tryptophan and Its Major Metabolites in Fluid from the Anterior Chamber of the Eye in Diabetic Patients with Cataract by Liquid Chromotography Mass Spectrometry (LC-MS/MS). *Molecules* **2018**, *23* (11), 3012.
(30) Raison, C. L.; Dantzer, R.; Kelley, K. W.; Lawson, M. A.; Woolwine, B. J.; Vogt, G.; Spivey, J. R.; Saito, K.; Miller, A. H. CSF concentrations of brain tryptophan and kynurenines during immune stimulation with IFN-alpha: relationship to CNS immune responses and depression. *Mol. Psychiatry* **2010**, *15*, 393−403.
(31) Kepplinger, B.; Baran, H.; Kainz, A.; Ferraz-Leite, H.; Newcombe, J.; Kalina, P. Age-Related Increase of Kynurenic Acid in Human Cerebrospinal Fluid−IgG and β2-Microglobulin Changes. *Neurosignals* **2005**, *14* (3), 126−135.
(32) Ilzecka, J.; Kocki, T.; Stelmasiak, Z.; Turski, W. A. Endogenous protectant kynurenic acid in amyotrophic lateral sclerosis. *Acta Neurologica Scandinavica* **2003**, *107* (6), 412−418.
(33) Adams, S.; Teo, C.; McDonald, K. L.; Zinger, A.; Bustamante, S.; Lim, C. K.; Sundaram, G.; Braidy, N.; Brew, B. J.; Guillemin, G. J. Involvement of the Kynurenine Pathway in Human Glioma Pathophysiology. *PLoS One* **2014**, *9* (11), No. e112945.
(34) Kepplinger, B.; Baran, H.; Kronsteiner, C.; Reuss, J. Increased Levels of Kynurenic Acid in the Cerebrospinal Fluid in Patients with Hydrocephalus. *Neurosignals* **2019**, *27*, 1−11.
(35) Zeng, R.; Qiu, M.; Wan, Q.; Huang, Z.; Liu, X.; Tang, D.; Knopp, D. Smartphone-Based Electrochemical Immunoassay for Point-of-Care Detection of SARS-CoV-2 Nucleocapsid Protein. *Anal. Chem.* **2022**, *94* (43), 15155−15161.
(36) Gao, Y.; Li, M.; Zeng, Y.; Liu, X.; Tang, D. Tunable Competitive Absorption-Induced Signal-On Photoelectrochemical Immunoassay for Cardiac Troponin I Based on Z-Scheme Metal−Organic Framework Heterojunctions. *Anal. Chem.* **2022**, *94* (39), 13582−13589.
(37) Song, Z.; Yuan, R.; Chai, Y.; Yin, B.; Fu, P.; Wang, J. Multilayer structured amperometric immunosensor based on gold nanoparticles and Prussian blue nanoparticles/nanocomposite functionalized interface. *Electrochim. Acta* **2010**, *55* (5), 1778−1784.
(38) Ou, C.; Yuan, R.; Chai, Y.; Tang, M.; Chai, R.; He, X. A novel amperometric immunosensor based on layer-by-layer assembly of gold nanoparticles−multi-walled carbon nanotubes-thionine multilayer films on polyelectrolyte surface. *Anal. Chim. Acta* **2007**, *603* (2), 205−213.
(39) Kiio, L. K.; Onyatta, J. O.; Ndangili, P. M.; Oloo, F.; Santamaría, C.; Montuenga, L. M.; Mbui, D. N. Development of electrochemical immunosensor for quantitative detection of non-small cell lung cancer (NSCLC) biomaker YES1. *Biosensors and Bioelectronics: X* **2023**, *14*, No. 100386.

https://doi.org/10.1021/acsmeasuresciau.4c00102
ACS Meas. Sci. Au 2025, 5, 242−249